Ablatively Cooled Pulse Rocket Engine Design

R. J. Fio Rito*
The Marquardt Corporation, Van Nuys, Calif.

The application of ablative cooling techniques to small hypergolic bipropellant pulse rocket thrust chambers is examined. The design and performance requirements for a typical control rocket are given. A systematic approach to an integrated engine design is delineated. Advanced materials under investigation are the high silica, asbestos, carbon, and zirconia-reinforced resin systems in addition to refractories and oxidation-resistant refractory coatings for nonablating thrust chamber sections. Ablative materials and refractory coating processes and control techniques are evaluated. Propellant injector aerothermodynamic effects on ablative chamber liners and the influence of pulse rocket duty cycle on over-all engine design are discussed. Empirical results of engines designed for space thrust levels of 25, 100, and 1750 lbf for short and long pulses varying from 10 msec to 10 min are compared with analytical predictions. Accumulated burning durations of 30 min and above have been demonstrated with thrust variations of less than ±1% at an average I_{sp} of 295 sec.

Introduction

THIS paper deals primarily with the application of reinforced plastics and oxidation-resistant ceramics to pulsed, thrust chambers for liquid-propellant rocket engines. Ablative cooling has been successfully employed for re-entry nose cone and relatively short-duration solid rocket nozzle liner applications. The work reported herein shows that the extension of this technology to long-life liquid rocket applications is feasible. The performance of an oxidation-resistant coating for graphite and various other high-temperature substrate materials is discussed as applied to liquid rocket ablative thrust chamber nozzle throat inserts. Excellent thermal shock and long life are indicated at operating temperatures in excess of 4000°F.

It is the intent of this paper to isolate and identify the important design considerations for ablative liquid rocket engines and to correlate test results with design criteria. The following aspects are evaluated: 1) effects of chamber geometry and injection hydrodynamics on heat transfer and boundary-layer control; 2) effects of orientation of reinforcement and composition of the reinforcement-resin system proportions on heat sink and structural characteristics, and criteria for the prediction of the heat sink capacity (char rate) of a reinforced plastic as a function of time for given thrust chamber environments; 3) the process control variables that affect thermal and mechanical properties of a thermosetting plastic, and a new approach for checking on the advancement of the resin cure; 4) the effect of ablation on the performance of a high expansion ratio (50:1) nozzle; 5) design techniques for effective injector-face to thrust-chamber sealing and thermal insulation; and 6) use of composite plastic systems to minimize thrust chamber weight.

Materials for Lining Pulsed Liquid Rockets

Materials for chamber linings for pulsed rocket engines fall into two general categories: 1) inorganic fiber-reinforced thermosetting plastics, and 2) refractory materials with relatively low surface erosion characteristics. In the first category, two design concepts involving ablative plastics have been considered for rockets:

1) A simple ablator that erodes into the main gas stream at a high rate can insulate the chamber wall and provide film cooling for the nozzle throat; this approach has been used successfully for the relatively short-duration (30 to 60 sec) solid rocket applications.

2) A reinforced char-forming plastic can act as a thermal insulator while forming a structurally sound, low-erosion-rate char layer in an intermittent high-temperature gas environment. This type shows more promise for pulsed hypergolic liquid rocket applications. The charring ablative process has been discussed in considerable detail in Refs. 1 and 2 and will not be repeated here, but heat-transfer aspects are discussed in a later section.

At the present time, knowledge of which resins are good char formers is largely empirical. Polyesters form porous chars that are mechanically weak.[3] Furthermore, the original plastic laminate matrix system is relatively weak and loses strength rapidly as temperature increases. Epoxy resins form strong laminates that retain an appreciable part of their strength to temperatures up to 300° to 350°F, but, unfortunately, do not form strong chars.[3,4] Modified epoxy resins have shown promise as good char formers. Systems based upon phenolic resins form strong, porous chars[4] and are currently favored for pulsed rocket application. The standard phenolic resins include SC 1008 (Monsanto Chemical Company), 91-LD (Cincinnati Testing Laboratory), and BLL-3085 (Bakelite Company). Reinforcing materials for these plastics have ranged in form from wound and chopped filaments to woven fabrics (linen and nylon), graphitized cotton, metal screens, and glasses. For liquid rocket chamber liners, woven fabrics of high-melting-point glasses (high-purity silica) currently appear to be best. The high-silica

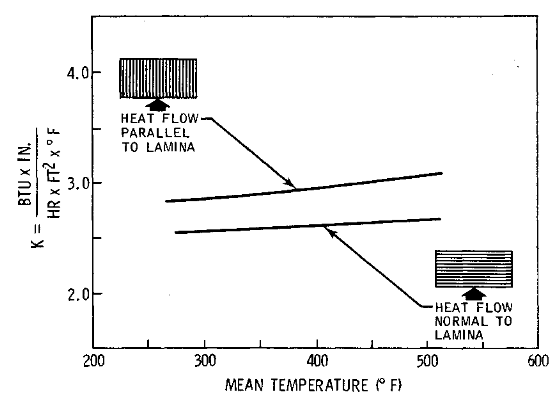

Fig. 1 Thermal conductivity of a silica/phenolic laminate.

Presented as Preprint 64-260 at the 1st AIAA Annual Meeting, Washington, D. C., June 29–July 2, 1964; revision received April 5, 1965. The consultation and assistance of C. D. Coulbert, B. A. Webb, M. D. Carey, J. W. Mitchell, and S. V. Castner of The Marquardt Corporation are gratefully acknowledged. Many of the test data shown were generated by the Advanced Product Development and Spacecraft Engine Groups of The Marquardt Corporation.

* Manager, Advanced Technical Staff. Member AIAA.

reinforcements include cloth and tape of Refrasil (H.I. Thompson Company), Sil-Temp (Haveg Industries), and Thermo-Sil (Aerothermal Industries, Inc.).

The physical and thermal properties of a reinforced plastic material depend on the basic materials, the proportions of plastic and reinforcement, the laminate orientation, and the processing variables. Effects of resin content and laminate orientation on thermal conductivity for a phenolic-glass laminate are shown in Figs. 1 and 2. Thermal conductivity is smaller in a direction normal to the laminations and tends to decrease with increasing weight fraction of resin. The data of Fig. 2 indicate that the thermal conductivity of the char is approximately one-half that of the original material and tends to increase with weight fraction of resin. These indications are questionable, however, since the decreased conductivity may be due to delamination voids which have been observed during torch tests of flat specimens. The latest firing test indications are that the conductivity of the char increases over that of the original material. Prior to testing the flight-type engine designs, numerous reinforced plastic materials were evaluated in small-scale (25-lbf thrust size) rocket firing tests. Calibrated injector and billet chambers at representative operating conditions were utilized. The results of these tests are shown in Table 1. Tests were also conducted at Marquardt to determine the effects of a high vacuum on the outgassing characteristics of a heated silica-phenolic laminate. The results are shown in Table 2. It is shown that negligible weight or dimensional changes occurred between the samples tested at vacuum and those tested at 1-atm pressure.

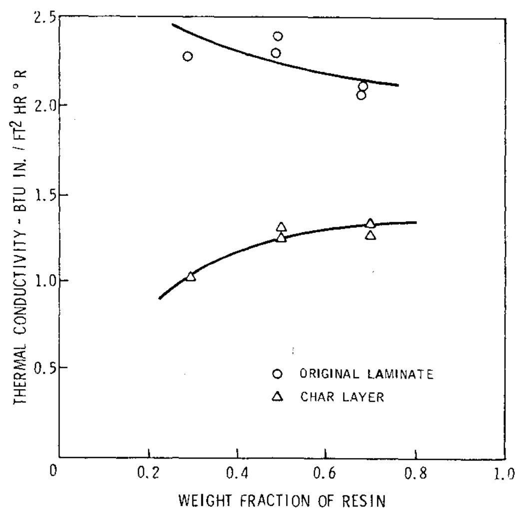

Fig. 2 Effect of resin content on thermal conductivity of phenolic-fiberglass laminate.

Table 1 Characteristics of reinforced plastics tested as chamber liners in billet chambers

Material (listed in order of over-all desirability)	Characteristics[a] Char rate	Erosion rate	Glassing	Delamination
Silica/phenolic laminates				
TMC-Fiberite MX 2646, 45° to ℄ (post cure)	2	2	1	1
TMC-USP FM 5067, 45° to ℄ (post cure)	1	2	2	2
TMC-Fiberite MX 2646, 60° to ℄ (post cure)	3	2	1	1
TMC-USP FM 5067, 60° to ℄ (no post cure)	2	2	2	2
TMC-USP FM 5504, 60° to ℄ (no post cure)	2	2	2	1
Hitco 1401 P, 30° to ℄ (no post cure)	2	2	3	2
Hitco 1401 P, 60° to ℄ (no post cure)	2	2	3	3
Hitco 1401 P, 90° to ℄ (no post cure)	3	2	4	3
Hitco resin 39, 90° to ℄ (no post cure)	1	2	2	4
Silica/epoxy Novolac laminates				
Avco X2001, 90° to ℄	4	1	2	4
Asbestos/phenolic nonlaminate				
Rheinhold PPD 150 $\frac{1}{2}$-in. chopped squares	1	4	1	...
Silica/phenolic nonlaminate				
Hitco XM-11 refrasil fiber	3	4	4	...
TMC-Fiberite MX 2646 $\frac{1}{2}$-in. squares	3	4	4	...
Rheinhold Fiberite MX 2625 $\frac{1}{2}$-in. squares	4	2	2	...
Carbon/phenolic Nonlaminate				
Rheinhold Fiberite MX 2630A $\frac{1}{2}$-in. squares	4	3	1	...
Zirconia/phenolic nonlaminate				
Hitco zirconia fiber	3	4	1	...
Nylon/phenolic				
Hitco/90° to centerline laminate	4	4	1	...
Rheinhold USP FM 5015 $\frac{1}{2}$-in. squares moulded	4	4	1	...

[a] Ratings: 1 = excellent, 2 = good, 3 = fair, 4 = poor.

The second thrust chamber liner material category consists of a refractory material (capable of high operating temperatures with low erosion) that is required in the nozzle throat, where a dimensional change can significantly affect engine performance. A refractory throat insert completely embedded in the thermally insulating plastic must be capable of operating at high surface temperatures (approaching gas temperatures) and must withstand the thermal shocks and vacuum ignition pressure shocks associated with pulsing engine operation. Many refractory materials have been evaluated, including the refractory metals, the metal oxides, carbides, silicides, and borides. These materials were evaluated under rocket firing conditions using the calibrated injector and billet chamber combination mentioned previously. Results of the test are tabulated in Table 3. The material combination giving the best over-all results to date has been a graphite substrate coated with an oxidation and thermal-shock-resistant, silicon carbide material designated Marquardt RM-005. This high-density, adherent, erosion-resistant coating material may be applied to the graphite to any desired thickness by a vapor deposition process that produces a very smooth, uniform, SiC layer. It can be applied at rates on the order of 0.060 in./hr. The coating produced is characterized by extremely high purity, fine grain size, and uniformity of composition; it is stoichiometric SiC and does not vary in composition from the surface to the substrate interface. The coating is formed independent of the substrate and results in a mechanical bond. The integrity of the bond is greatly improved by a special pretreatment of the graphite substrate.

The type of graphite substrate used is an important factor in the successful performance of the coating. Since most commercial graphites are anisotropic, thermal cycling results in crack formation in the coating due to differences in the thermal expansion. This problem is virtually eliminated through the use of isotropic graphites with a linear expansion very nearly the same as that of the vapor-deposited silicon carbide. This factor also dictates the other refractory substrates to which this coating can be applied; tungsten is the most suitable refractory metal presently available for use with this coating. This SiC coating is very resistant to oxidation and erosion in a high-velocity gas stream. To qualita-

Table 2 High-temperature degradation of laminated refrasil-phenolic material[a] in a vacuum environment

Run no.	Environment	Run time, min	Lamina orientation to axis	Maximum surface temp., °F	Maximum back face temp., °F.	Weight loss, %	Length change, %	Outer diameter change, %	Inner diameter change, %
1	Vacuum[b]	4	Perpend.	2340	...	12.0	+2.4	−1.96	−1.94
2	Vacuum	4	Parallel	2580	...	13.3	−2.02	−0.25	+5.5[c]
3	1 atm	4	Parallel	2440	...	11.8	−0.45	+0.3	−0.2
4	1 atm	4	Perpend.	2580	...	11.4	+0.077	−1.04	−0.75
5 (rerun of 1)	Vacuum	3	Perpend.	...	1143	1.67	0	−0.05	+0.1
6 (rerun of 4)	1 atm	3	Perpend.	...	1155	1.3	+0.31	0.25	+0.6

[a] Laminated refrasil phenolic cylinders, approximately 2-in. o.d., 1-in. i.d., and 1.25-in. length.
[b] Maximum vacuum: 10^{-3} mm Hg; all samples were soaked in environment for 2 hr. after firing.
[c] Large dimensional change in run 2 was due to cracking of sample.

tively screen the material prior to rocket firing evaluation, a series of laboratory oxidation tests was conducted using oxidizing, oxyacetylene flame. Coated test bars of both tungsten and graphite were subjected to temperatures of 3400° to 3600°F for extended periods of time with multiple thermal cycles with no observed changes in the appearance of the test part. Table 4 summarizes some of the oxyacetylene torch tests on silicon carbide coated substrates.

Design Integration

As in other rocket engine systems, the successful ablative rocket design is a balance of good mechanical design, application of thermodynamic principles, and proper use of materials. It is necessary, by proper thermodynamic design, to minimize convective heat transfer to the ablative materials and thus maximize the cooling capacity to chamber weight ratio. The design areas involved are the injector, the combustion chamber, and the nozzle. These three component areas will be briefly discussed in the following. In addition, heat transfer, quality control for reinforced plastics, and effects of the engine duty cycle will be covered.

Injector

In addition to bringing together the liquid propellants in the proper proportion for stable, efficient combustion, the injector in an ablatively cooled rocket must: 1) be designed to expose the minimum face area for radiant heat transmission from the hot chamber walls during shutdown periods, 2) provide a uniform fuel-rich (reducing) film adjacent to the chamber wall boundary layer, 3) eliminate high-velocity gas impingement on the chamber walls, and 4) prevent raw oxidizer impingement on hot chamber walls during pulsing operation. Requirements 2 and 4 stem from experimental observations of severe erosion of the chamber wall arising from direct oxidizer impingement or lack of a fuel-rich boundary layer when the injector resultant momentum angle is directed toward the wall. It is hypothesized that this effect, caused by local exothermic reaction of the ablating gases with the oxidizer, resulting in disruption of the boundary layer and the formation of high-shear-force "hot spots," with a consequent decrease in viscosity coupled with the increase in shear force, tends to sweep the liquid-phase silica from the chamber wall.

Combustion Chamber

The combustion chamber liner section is shown in Fig. 3. For the typical pulse rocket (100-lbf space thrust size), the chamber is quite short (2 to 4 in.) with L^* values ranging from 8 to 12 in. The short length enables a fuel-rich boundary layer to be propagated from the injector to the throat and to minimize convective heat transfer at the critical region. To absorb the thermal and structural loads in the most efficient manner, the combustion chamber section is a molded plastic composite consisting of a laminated reinforced plastic core with a higher-strength structural plastic circumferentially laminated outer shell molded integrally to the central core. The core section laminations are edge-oriented to the gas flow to provide the most efficient utilization of core volume as a heat sink. The laminated plastic exhibits anisotropic properties (higher thermal conductivity parallel to laminations); it also appears to have a higher effective specific heat parallel to the laminations. The laminations may, therefore, be oriented so as to provide maximum heat-sink volume at the region of highest heat flux (nozzle throat) and minimum conductivity where the minimum operating temperatures are required (e.g., injector face seal).

The cooling core must degrade (char) at a minimum rate, and the char must retain sufficient structural integrity to resist high mass removal from combustion gas shear forces. Laminate orientation angle does not have a noticeable effect on char rate in the orientation range from 90° to 45°. A greater tendency toward delamination exists at the higher orientation angles (90°). The high-purity silica phenolics

Table 3 Characteristics of throat-insert materials tested in billet chambers

Material (Listed in order of over-all desirability)	Characteristics[a]		
	Thermal shock	Erosion	Coating bond
Coated graphites			
TMC-005/La Carbonne grade P2239			
Coating process B	1	1	1
TMC-005/Carbon Products Div., Union Carbide Corp.			
Coating process B	1	2	1
TMC-005/Great Lakes HLM			
Coating process A	2	1	3
TMC-005/Graphite specialties grade G			
Coating process A	2	2	3
Nerghlo diffusion coat SiC/ Graphite specialties grade G	2	3	3
Rokide Z/LA Carbonne P5890	2	2	4
Teleflex tungsten/La Carbonne P5890	2	4	2
Reinforced plastic laminates			
Avco epoxy Novolac (X2001), 90° to centerline	1	3	...
TMC-Fiberite MX 2646, 45° to centerline	1	3	...
TMC-USP FM 5067, 45° to centerline	1	3	...
Refractories			
Kennametal (titanium carbide)	4	3	...
Pure tantalum	1	4	...
Sintered tungsten	1	4	...

[a] Ratings: 1 = excellent, 2 = good, 3 = fair, 4 = poor.

have exhibited the best thermal and mechanical properties to date. The graphite-reinforced phenolics tend to char and erode rapidly in an oxidizing atmosphere. In addition, the graphite-reinforced plastics have a greater tendency toward blowing (heavy delamination) in the char due to the large volume of gas products released from the combination of resin pyrolysis and oxidation of the carbon reinforcement. Zirconia reinforcements have been disappointing because of excessively high erosion rates. To date, zirconia fibers cannot be successfully woven or processed to produce a matrix capable of good char retention.

The outstanding advantage of the silica reinforcement is its capability to be woven into a high-strength cloth that provides good char retention. Silica is oxidation-resistant and stable for the temperature range of interest. High-purity silica (over 98%) has a transition melting point of 3100°F and remains highly viscous up to 4600°F. The silica-phenolic combination therefore provides a two-component heat sink capability. The endothermic pyrolysis of the organic resin is initially effective in the low temperature range (600° to 1500°F). The silica enters a gradual transition from solid to liquid at 3100°F; a second, more significant heat sink capability comes into effect when the silica reaches melting temperatures and reacts with carbon.[1] The glassy silica melt remains highly viscous and therefore resistant to shear forces over a significant temperature range.

Composite Designs for Exhaust Nozzles

The nozzle throat section is of particular importance because variations in throat area affect the thrust output of the engine; for a constant-propellant-supply-pressure system, an increase in throat area increases thrust and decreases specific impulse. Furthermore, the smaller the engine, the greater will be the area change for a given surface recession rate. It is necessary, therefore, to consider a nonablating throat material for long operational life pulsed rocket engines. The material must be resistant to thermal shock and to the chemical environment produced by the combustion gases and the products of ablation and must withstand extended exposure at surface temperatures of 3500° to 4000°F. Many refractory materials and oxidation-resistant coatings have been evaluated. The best results having been obtained with the SiC coating previously discussed. Particular attention must be given the interface design between the nonablating throat insert and the reinforced plastic insulation. The insert is incorporated in the plastic molding process and bonded to the plastic with an epoxy-phenolic resin mixture. Since the region of maximum heat flux occurs in the convergent section of the throat, the insert must be designed with an approach section such that the joint between the insert and plastic is sufficiently upstream of the throat to avoid an excessive local erosion rate of the plastic. It is also important to observe empirical relationships between imbedded depth of the insert and gas leakage around the outer diameter of the insert, which can, in extreme cases, cause complete expulsion of the insert. Maximum use must be made of the throat insert's heat-sink capabilities to minimize the transient temperatures attained at the insert inner surface. The expansion section is a continuation of the laminated edge-oriented plastic core section (Fig. 3). It can be either a continuous plastic ribbon winding molded to the throat insert or a separate die-molded plastic billet that is machined to accept the insert with an integral bonded joint to the forward billet.

Table 4 Performance of TMC RM-005 coating in oxyacetylene torch test

Substrate, dimensions, in.	Coating in.	Temp., °F	Time, min.	Remarks[a]
W strip	0	3400	2	*B*
½ × 6 × 0.040	0.020	3200	360	*TT*
	0.034	3400	420	*TT*
	0.023	3600	60	*E*
Ta-10W strip	0	3250	2	*B*
½ × 6 × 0.040	0.010	3600	36	*C*
Mo cylinder	0	3000	2	*B*
2 (diam) × 3 × 0.060 wall	0.006	3100	120	*TT*
Graphite bar	0	3000	10	*B*
¼ × 1 × 4	0.020	3200	360	*TT*
	0.020	3400	360	*TT*
	0.020	3600	60	*TT*

[a] *B* = complete burnthrough, *TT* = no failure; test terminated, *E* = bottom edge failure, *C* = cracked during thermal cycle.

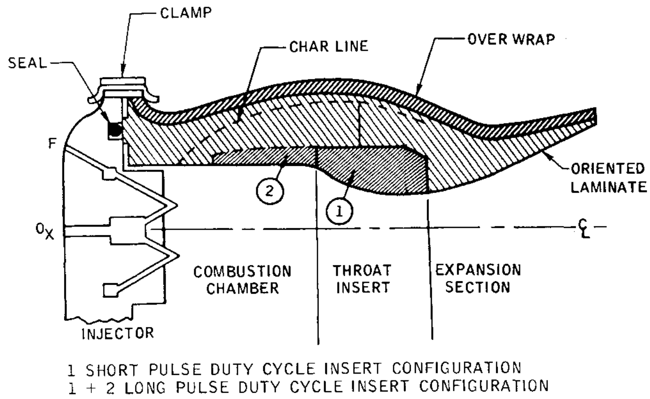

Fig. 3 Typical ablative hypergolic pulse rocket engine.

Heat-Transfer Analysis

To provide an analytical approach for predicting transient thermal behavior in a silica phenolic material, a transient temperature analysis was formulated using convective film heat-transfer coefficients from the Bartz equation[5] and one-dimensional heat conduction in a pipe. The analytical model giving the material thermal properties (assumed to remain constant), and the combustion gas conditions are shown in Fig. 4. This model represents the 1750-lbf engine. The calculations were programmed on the IBM 704 Thermal Analyzer, and the analytical results are shown in Figs. 5 and 6. Figure 5 shows a rapid rise in inner wall temperature transient to a nearly constant value of from 4400° to 4600°F. Figure 6 shows reasonable agreement between calculated temperature transients at various depths from the inner surface and corresponding thermocouple data from 1750-lbf engine tests.

Theoretical relationships for the prediction of char rate in ablative rocket thrust chamber liners where erosion is neg-

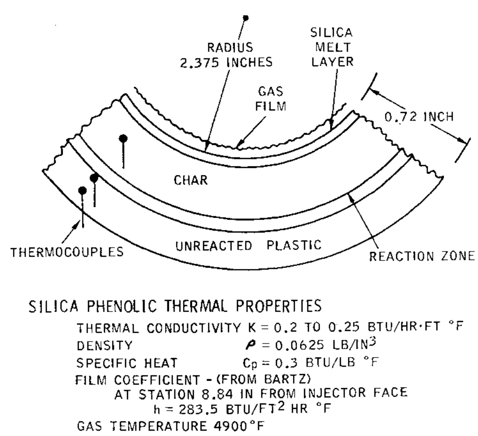

Fig. 4 Analytical model for transient-temperature analysis of chamber liner of edge-oriented silica/phenolic laminate.

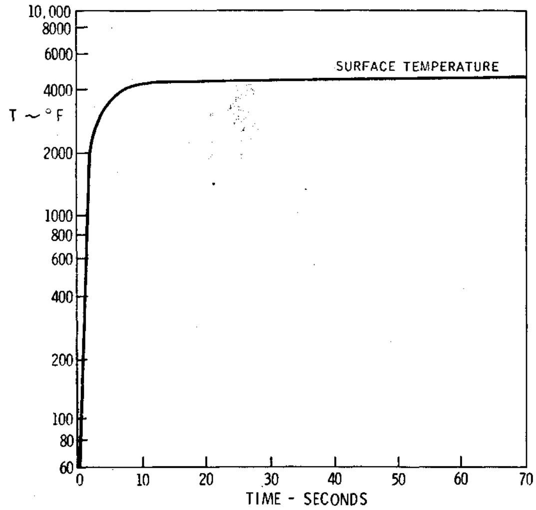

Fig. 5 Inner surface temperature vs time for model of Fig. 4.

ligible have been studied by various investigators. Green[6] shows the relationship, $d = Ct^{1/2}$, where d is the char depth (inches), C is a constant (for a given material), and t is the combustion time (seconds). Test data from various sources are shown in Fig. 7, together with theoretical curves based upon one-dimensional heat conduction theory for 1) an infinite slab and 2) a thick-walled cylinder having an internal diameter of 1.2 in. and an outer diameter of 4.0 in. It was assumed that the internal wall temperature was maintained at 4300°F and that the thermal properties were as given for the model of Fig. 4 and did not vary with temperature. The predicted curves for the slab and the thick-walled cylinder are in close agreement, and both follow the $t^{1/2}$ relationship. This slope is reasonably good for all sets of test data. The spread among sets is to be expected, since the data were taken for a variety of engine sizes (0.3- to 4.0-in. throat diam), material variations, and operating conditions. In general, the data for larger engines fall on or below the curves, whereas the short-pulse duty cycle data from the Marquardt tests fall above the curves, showing erosion rates approximately 1.5 to 2 times higher.

Material Process and Quality Control

An important factor influencing the thermal and mechanical properties as well as the reproducibility of the reinforced plastics is the precise control of the processing variables. The purity of the silica-reinforcing medium must be

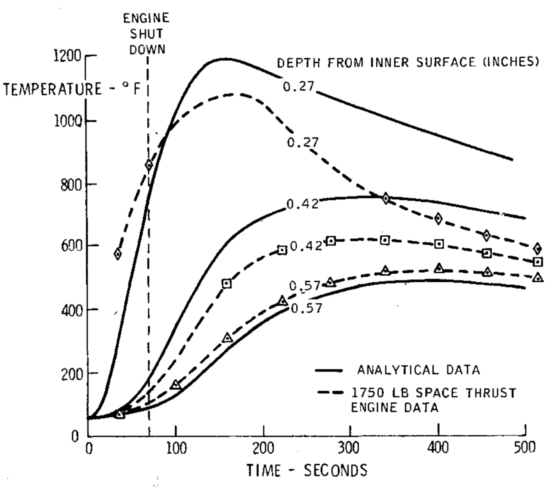

Fig. 6 Predicted and measured temperature histories at various depths for 1750-lbf-thrust engine.

Table 5 Typical hypergolic pulse rocket performance and design requirements

Propellants: N_2O_4-mixed amines,
Duration:
Pulsing duty cycles:

Thrust, lbf	% ON	Frequency, cps	Total ON time, sec
25, 100	20	10	300
1750	25	0.05	180

Continuous: 25 or 100 lbf for 10 min (max).
Thrust (space): 25, 100, 25, 100, 1750 lbf,
Specific impulse: ≥ 300 sec at $A_e/A_t = 40$.
Engine thrust/weight ratio: ≥ 10.
Maximum outer surface temperature: thrust chamber = 500°F, injector head = 200°F, injector valves = 150°F.

maintained at a high value (98% or better) in order to obtain high melting temperatures and high melt viscosity. Small amounts of impurities containing the alkali metals act as fluxes to reduce the silica melting temperature. The composition of the resin system must be controlled, as well as the degree of cure of the thermosetting plastic as a prepreg during the molding process. Materials control investigations are important to plastic fabrication because the condition of the "prepregs" (resin impregnated fabrics and partially cured) at the time of receipt and at the time of molding controls the ease of part fabrication and the quality of the molded parts.

A polymerization index based on infrared spectrophotometric measurements has been developed which has all of the desired qualities of a routine control test. The infrared procedure essentially indicates the disappearance of reactive sites on the resin benzene ring. Previous experiments have disclosed that a resin advances in molecular weight (cure advancement) through cross-linking at reactive sites on the benzene nucleus. Surveillance of the variation in sites is an index of the actual state of advancement of the resin. The reactive sites consists of methylol groups (CH_2OH) and are identifiable on the infrared absorption spectrum at a wavelength of 9.8 μ. As the resin is advanced, the reactive sites are converted into methylene and ether linkages connecting the benzene nucleus in a three-dimensional network, which, if carried to the C-stage (completely cured resin), approaches an infinite molecular weight.

Acetone is used as a solvent to extract a resin sample at various stages in the prepreg storage or fabrication process.

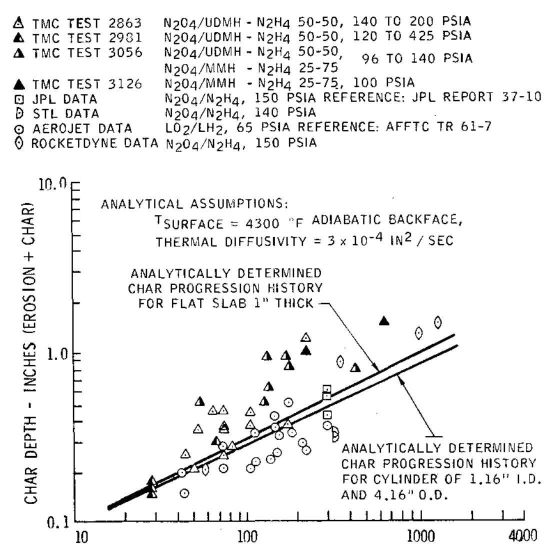

Fig. 7 Compilation of test data for refrasil-phenolic char depth vs burning time.

Table 6 Detailed performance of 37.5-, 100-, and 1750-lbf-space-thrust engines; N_2O_4 and 50/50 UDMH-N_2H_4 propellants for all engines

Item	Engine: 37.5 lbf no. B-1	100 lbf short pulse no. C-7	100 lbf long pulse no. C-9	1750 lbf no. D-15
Duty cycle accomplished, (time on(sec)/time off(sec))$_{\text{no. of cycles}}$	$(10/600)_1$ $(13/200)_{20}$	$(5/300)_3$ $(180/300)_3$ $(10/180)_4$ $(1/1)_6$ $(5/3600)_1$ $(10/\infty)$	$(5/300)_2$ $(6/5)_3$ $(71/1500)_1$ $(2/60)_3$ $(202/15600)_1$ $(314/\infty)$	$(5/5)_1$ $(10/12)_1$ $(30/15)_1$ $(10/15)_2$ $(40/10)_3$ $(75/\infty)$
Total duty cycle; on time, sec	270	426	621	262
off time, sec	4400	2285	18237	5580
P_∞, psia	≤ 0.035	≤ 0.12	≤ 1.5	≤ 1.5
O/F Ratio	1.6	1.45	1.49	1.62
P_c psia	151	148	143	157
Expansion ratio	35/1	47/1	5.5	2.4
Delivered thrust, lbf	37.5	100 ± 1	82.5	1200
I_{sp}, sec, max	312	301	253	...
min	303	294	244	...
avg	304	293	250	298 ($\epsilon = 20$)
L^*, in.	9.8	11.5	7.6	34
Throat diameter erosion, in.	Zero	Zero	0.0022	Zero
Max temperature,[a] °F	300	See Fig. 10	Ch. wall 700 Inj. hd. 356	See Fig. 10
Engine weight (not optimized for duty cycle), lb	...	15.3	....	....

[a] Soakback after completion of duty cycle.

Corrections are made for concentration dependence of the acetone solution by correlation with known significant absorption bands in the infrared spectrum.

The band at 12.2 μ consisting of disubstituted phenol groups is used as an internal standard of comparison because of its stability and low free-phenol sensitivity. The index of cure is established by the ratio of 12.2 μ absorbance to 9.8 μ absorbance. This 12.2/9.8 ratio produces an index number that increases with the increase in advancement in cure.

Duty Cycle

As indicated by the requirements of Table 5, the typical pulse rocket engine must operate over a wide range of duty cycles ranging from 10-msec pulses of thrust to continuous burning periods up to 10 min. It is of interest to consider the influence of operational mode on ablative thrust chamber design considering two basic modes: 1) short pulse ≤ 120 sec cumulative thrust time at 10 to 15% duty cycle, and 2) single long pulse (continuous, >120 sec). Test data have shown that the long-pulse duty cycle is less severe from a charring standpoint in the region of the combustion chamber and throat insert but more severe in the region of the nozzle expansion section. The short-pulse operational mode primarily affects the organic constituents of the reinforced plastic and results in a higher char rate for the following reasons: 1) the convective heat flux to the plastic walls is higher because average wall temperatures are lower in cyclic operation $[q/A = h(T_g - T_w)]$, and 2) heat absorbed by the charred material and throat insert must be dissipated during cooldown primarily by conduction to the unreacted plastic. The radiation losses to the injector face are relatively insignificant. This increment of heat multiplied by the number of cooldown cycles, then, is the heat load conducted to the reaction zone for advancement of the char.

Test Results: Flight-Type Engine Performance

The 37.5-lbf space-thrust pulse engine consisted of a non-weight-optimized thrust chamber with a flight-type injector and a high-expansion-altitude nozzle. The detailed performance for a short-pulse duty cycle is shown in Table 6.

Detailed performance for a 100-lbf space-thrust, flight-type, short-pulse engine is given in Table 6. This engine successfully accomplished its duty cycle with no measurable erosion from either the chamber liner or throat insert. A photograph of the engine after test is shown in Fig. 8. The engine was in good structural condition after the run. There were no indications of leakage at the injector to thrust chamber joint.

Performance for a flight-type, long-pulse, 100-lbf space-thrust engine is shown in Table 6. The detailed design of the throat insert for this engine differed from that of the short-pulse engine. The engine successfully completed the duty cycle with negligible liner or throat erosion. The char depth of the outer plastic insulation had extended to the asbestos overwrap in the plane of the throat where the maximum outer wall temperature of 700°F had been attained.

Engine D-4 was a hard-throat, sea-level, flight weight configuration with 1750-lbf thrust. It was tested on a short-pulse duty cycle. This chamber incorporated a fiberglass-filament-wound outer structural shell over a parallel wrap

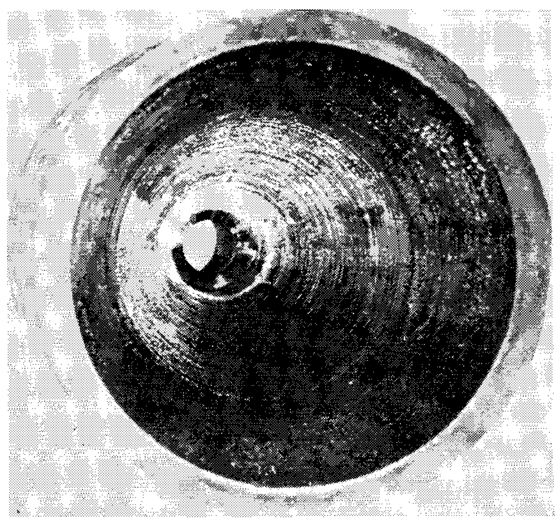

Fig. 8 Exit nozzle section of 100-lbf-thrust, flight-weight rocket engine after 420 sec of operation.

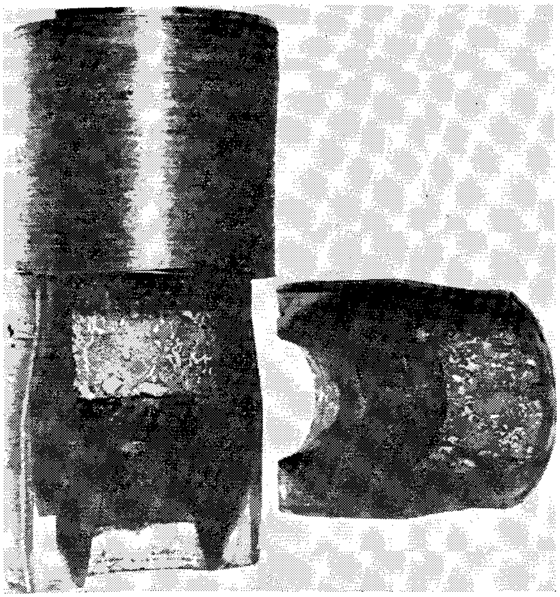

Fig. 9 Section of flight-weight, 1750-lbf-space-thrust engine after test.

insulating layer. The detailed performance summary is given in Table 6. Postrun sectioned views of the chamber are shown in Fig. 9.

Concluding Remarks

Of the ablative materials evaluated to date, best results† for pulsed-rocket chamber liners are 1) a silica-cloth-reinforced nylon modified phenolic laminate that is compression molded and postcured (Marquardt Fiberite MX 2646), and 2) a silica-cloth-reinforced modified phenolic laminate that is compression molded but not postcured (Marquardt USP FM 5067).

Best refractory material performance for noneroding hard-throat inserts was obtained with a vapor-deposited oxidation-resistant SiC coating (Marquardt RM005) on substrates of graphite (La Carbone and Carbon Products Division, Union Carbide Corporation).

Long-pulse duty cycles (greater than 120 sec) induce more severe erosion on a silica liner than a series of shorter pulses. A combination throat and partial chamber liner of refractory is required to minimize liner and throat erosion.

Empirical and analytical char rate data for radial heat flow in rocket thrust chambers show universal agreement with an expression relating char depth to time to the one-half power. Reasonable correlation with transient test data were obtained

† These results apply to the integrated injector-chamber configuration, propellants, and operating conditions specified herein, since material performance is strongly dependent on these combined factors.

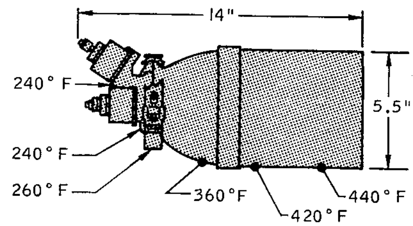

a) 100-lbf space thrust, short-pulse engine C-7

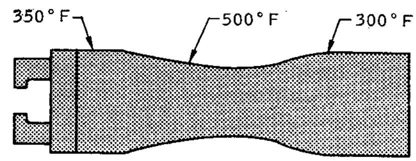

b) 1750-lbf space thrust, short-pulse engine D-15

Fig. 10 Detailed engine performance; maximum external temperatures.

using conductive heat-transfer theory for thick-walled pipes. Lack of accurate thermal property data for the plastic materials was a handicap in the analysis.

Successful demonstration of an integrated‡ design concept for an ablative hypergolic pulse rocket for space uses was demonstrated for 25-, 100-, and 1750-lbf sizes. The following duty cycles were demonstrated: short-pulse cycles with firing durations up to 480 sec at 298-sec average I_{sp}; long-pulse duty cycles with firing durations up to 621 sec at an average I_{sp} of 300 sec; and combined long- and short-pulse cycles with firing durations up to 1200 sec at an average I_{sp} of 295 sec.

References

[1] Beecher, N. and Rosensweig, R. E., "Ablation mechanisms in plastics with inorganic reinforcement," ARS J. **31**, 532–539 (1961).

[2] Scala, S. M. and Gilbert, L. M., "The thermal degradation of a char forming plastic during hypersonic flight," ARS Paper 2100-61 (October 1961).

[3] Lapple, C., "Mechanisms of ablation of char forming ablative plastics," Aeronautical Systems Div. TR 61-204 (1961).

[4] Friel, P. J., "Ablation of thermosetting plastics," Planetary Space Sci. **3**, 83–84 (1961).

[5] Bartz, D. R., "A simple equation for rapid estimation of rocket nozzle convective heat transfer coefficients," Jet Propulsion Lab., pp. 49–51 (January 1950).

[6] Greene, R. B., "The surface ablation of fiber reinforced plastics parallel to an oxy-acetylene flame," Univ. of Calif. Eng. Project Rept. H. E. 150-179 (February 1960).

‡ Integrated design makes maximum use of the high-temperature material properties by integration of injector and thrust chamber aerothermodynamic design in achieving reduced heat flux to the chamber walls by boundary-layer control.